Electronic Supplementary Material (ESI) for Dalton Transactions.

SUPPORTING INFORMATION

Influence of Aluminum Zoning Toward External Surfaces in MFI Zeolites on Propene Oligomerization Catalysis

Ricem Diaz Arroyo, Young Gul Hur, and Rajamani Gounder*

Charles D. Davidson School of Chemical Engineering, Purdue University, 480 Stadium Mall Drive, West Lafayette, IN 47907, USA

*Corresponding author: e-mail: rgounder@purdue.edu

Table of Contents

Section S1. Materials and Methods

1.1. Synthesis of MFI zeolites

Samples are named MFI-X-Y, where X denotes the average crystallite size in nm, and Y denotes the crystallite-scale Al distribution (Z = zoned, H = homogeneous).

For the synthesis of MFI-183-Z (core@shell), MFI-208 (Si-MFI) was used as the seed material and was synthesized adapting a procedure reported elsewhere.[1] A synthesis gel molar composition of 1 SiO_2/0.24 TPAOH/0.004 Na_2O/40 H_2O was prepared by dissolving tetraethyl orthosilicate (98%, Sigma, TEOS) in a solution of tetrapropylammonium hydroxide (40%, Alfa Aesar, TPAOH) and deionized (18.2 MΩ cm, DI) water. The solution was stirred overnight at ambient temperature. The ethanol formed from hydrolyzing TEOS was not purposefully evaporated from the synthesis solution. The synthesis solution was transferred to a Teflon-lined stainless-steel autoclave (Parr Instruments) and heated at 373 K in a static oven for 60 h. The solid products were washed 3-4 times with DI water until the pH was 7. The gel was separated by centrifugation at 5000 rpm, and the supernatant was decanted. Solid products were dried in a static oven overnight at 373 K. The MFI-208 seed material was transferred to a second synthesis gel with molar composition of 1 SiO_2/0.2 TPAOH/0.04 Na_2O/0.03Al_2O_3/400 H_2O, as previously reported.[2] This gel was prepared by dissolving aluminum sulfate ($Al_2(SO_4)_3 \cdot 18H_2O$, 98%, Sigma) in an aqueous solution of TPAOH and NaOH, followed by adding tetraethyl orthosilicate (98%, Sigma, TEOS). The mixture was stirred for 2 h at ambient temperature before the Si-MFI seeds were added to obtain a 10 wt% suspension. The synthesis was performed under rotation (60 rpm) at 393 K for 48 h.

MFI-158-H (Al-MFI) was synthesized following a procedure reported elsewhere.[3] A synthesis gel molar ratio of 1 SiO_2/0.24 TPAOH/0.004 Na_2O/0.10 Al_2O_3 /19.20 H_2O was prepared

by dissolving tetraethylorthosilicate (98%, Sigma, TEOS) was dissolved in a solution of tetrapropylammonium hydroxide (40%, Alfa Aesar, TPAOH), sodium hydroxide pellets (98%, Sigma, NaOH) and DI water. The solution was stirred overnight at ambient temperature. Aluminum isopropoxide (98%, Sigma) was added and stirred for 24 h at ambient temperature. The synthesis solution was placed in a Teflon-lined stainless-steel autoclave (Parr Instruments) and heated at 373 K in a static oven (Yamato DKN-402C) for 60 h. The solid products were washed 3-4 times with DI water until the pH was 7. The solid was separated by centrifugation at 5000 rpm, and the supernatant was decanted.

MFI-22-H was synthesized using a gemini-type quaternary ammonium surfactant (C_{666}, $C_6H_{13}{-}N^+(CH_3)_2{-}C_6H_{12}{-}N^+(CH_3)_2{-}C_6H_{13}{\cdot}2Br^-$), which was prepared following previously reported methods.[4] A synthesis gel was prepared with molar ratios of 1 SiO_2/0.18 NaOH/0.010 $Al_2(SO_4)_3$/0.10 C_{666}/40 H_2O. To prepare the synthesis gel, 1.68 g of C_{666}, 2.40 g of sodium hydroxide solution (10 wt/wt % NaOH, Sigma-Aldrich, 97 wt % in deionized H2O), and 13.7 g of DI water were combined and stirred until homogenized in a PFA jar. In a separate PFA jar, 0.22 g of aluminum sulfate octadecahydrate ($Al_2(SO_4)_3{\cdot}18H_2O$, Sigma-Aidrich, ≥97%) was dissolved in 5 g of DI water. The aluminum sulfate solution was added dropwise to the first solution. Finally, 5.01 g of colloidal silica (Ludox AS40, 40 wt/wt %, Sigma-Aldrich) was added to the mixture and stirred for 12 h under ambient conditions. The synthesis solution was then transferred to a 45 cm^3 Teflon-lined stainless-steel autoclave and placed in a forced convection oven at 403 K for 7 days under rotation (60 rpm). Solids were recovered via centrifugation at 8,000 rpm and washed with deionized water until the pH of the supernatant reached a value below 8.

1.2. Characterization of MFI zeolites

Crystal structures were determined using powder X-ray diffraction (XRD) patterns obtained from a Rigaku SmartLab X-ray diffractometer with a Cu Kα radiation source (λ = 1.54 Å, 40 kV, 44 mA). The diffraction patterns were measured from 2θ of 4° to 50° with a step size of 0.01° and a scan rate of 0.0167° s^{-1}.

N_2 adsorption isotherms were measured at 77 K using a Micromeritics 3-Flex. Approximately 0.05 g of samples were evacuated under dynamic vacuum (<0.67 KPa), heated to 393 K for 2 h, followed by heating to 623 K for 9 h (0.167 K s^{-1}) before the adsorption measurement. Micropore volumes of the samples were determined by finding the minimum of the semilogarithmic plot of $\partial(V_{ads})/ \partial(\ln(P/P_0))$ versus $\ln(P/P_0)$ and by extrapolating the uptake of liquid N_2 (P/P_0 = 0.05-0.9) on degassed samples to zero pressure. Micropore volumes estimated by both methods agreed within ± 5%.

Elemental compositions of samples were analyzed using inductively coupled plasma-optical emission spectroscopy (ICP-OES) measurements with a Thermo Scientific iCAP 7000 Plus Series ICP-OES. Aqueous samples were prepared by dissolving ca. 0.02 g of solid in 2.5 g of hydrofluoric acid (48 wt %, Alfa Aesar). After >24 h, 1 g of HNO3 (70 wt %, Sigma-Aldrich) was added and diluted with 50 g of deionized water. [*Caution: when working with HF acid, use appropriate personal protective equipment, ventilation, and other safety precautions*].

To remove the organic material from as-synthesized samples, typically ca. 0.02 g of the as-synthesized sample was heated in flowing dry air (1.67 cm^3 s^{-1}, 99.999% UHP, Indiana Oxygen) to 373 K (0.167 K s^{-1}), held for 0.5 h, heated to 1073 K (0.167 K s^{-1}), and held for 0.5 h to combust the organic content.

Crystal morphology and particle size distributions of the core and core@shell materials were assessed by scanning electron microscopy (SEM) on FEI Quanta 3D FEG Dual-beam SEM operated at 5 kV and a spot size of 3. SEM samples were prepared by adding a small amount of zeolite in an aqueous solution and vortexing for 180 s. Droplets of this mixture were deposited onto carbon tape and coated with a thin layer of carbon to prevent charging effects during image collection. Transmission electron microscopy (TEM) images were recorded in a Talos F200X instrument with high-resolution TEM and scanning TEM, operating at an accelerating voltage of 300kV coupled with energy dispersive X-ray spectroscopy (EDX) after mounting the samples on a carbon grid (300 mesh) using methanol dispersion with sonication for 180 s.

The H^+ content of each sampls was quantified by ammonia temperature programmed desorption (NH_3-TPD) of NH_4^+-form samples on a Micromeritics AutoChem II 2920 Chemisorption analyzer and an Agilent 5973N mass selective detection (MSD) system. NH_4-form samples were prepared by aqueous ion exchange in a 1 M NH_4NO_3 solution (100 $cm^3\ g_{sample}^{-1}$, $NH_4NO_3 \geq 98\%$, Sigma-Aldrich, 24 h, ambient temperature). Exchanged samples were washed with deionized water (30 $cm^3\ g_{sample}^{-1}$, 4×) and dried overnight at 373 K in stagnant air. In TPD experiments, NH_4-form samples were held at 323 K for 0.5 h under flowing He (∼1 × 10^{-5} mol s^{-1}, 99.999%, Indiana Oxygen). The temperature was increased to 873 K (at 0.167 K s^{-1}) while quantifying the NH^3 desorbed.

X-ray photoelectron spectroscopy (XPS) was performed at the Surface Analysis Facility of the Birck Nanotechnology Center (Purdue University) using a Kratos AXIS Ultra DLD Imaging spectrometer equipped with a standard achromatic Al Kα X-ray source (1483.6 eV) operating at 75 W and 12 minutes of acquisition time. The data were acquired while the sample was under high vacuum (P ∼ 10–9 Torr) analyzed with CasaXPS software (version 2.3.25PR1.0) and the binding

energies on each sample were corrected for surface charging effects by setting the C 1s peak of the adventitious carbon to a binding energy of 284.8 eV. Surface elemental composition (Si/Al) was quantified using the integrated areas of the Si 2p and Al 2p peaks and the Scofield photoionization cross sections.

1.3. Mesitylene benzylation kinetics studies

The experimental procedure for mesitylene benzylation in a batch reactor was adapted from prior literature.[5–7] All liquid reactants were used as received and without further purification. The proton form of a specified pellet size of MFI catalyst (50–200 mg) was converted from the NH_4-form MFI samples by treating in flowing dry air (1.67 $cm^3\ s^{-1}\ g_{zeolite}^{-1}$, 99.999% UHP, Indiana Oxygen) to 773 K (0.0167 K s^{-1}) in a muffle furnace (Nabertherm) and holding for 4 h. H-form zeolite samples were pelleted, crushed and sieved into 125-250 μm aggregates. The catalyst sample and a PTFE magnetic stir bar (VWR) were added into a 10 mL thick-walled glass batch reactor (VWR). Then, the reactor was sealed with a crimped cap (PTFE/silicone septum, Agilent) and placed in an oil bath while stirring at 900 rpm. The catalyst was heated to 423 K (~1 K s^{-1}) and held for 1 h to desorb residual water from the solid, and then a needle was used to pierce the septum to relieve pressure. The batch reactor containing the catalyst was then cooled to reaction temperature (363 K).

In a separate 10 cm^3 thick-walled glass vial on an heated stir plate, mesitylene (～6 cm^3, ≥99.0%, Thermo Scientific) was preheated to 363 K for 0.5 h, and then 5.0 cm^3 of preheated mesitylene was transferred using a 2.5 cm^3 glass syringe (Hamilton) into the batch reactor containing the preheated catalyst at 363 K. The batch reactor containing the catalyst and mesitylene was heated for another 0.5 h at 363 K under stirring (900 rpm). Approximately 0.1 cm^3 aliquot

was taken after 0.5 h to confirm no self-reaction of mesitylene occured (e.g., isomerization or transmethylation). The reaction was initiated by injecting with a 6" needle (Kemtech America) 0.4 cm^3 of dibenzyl ether (DBE, 99%, Thermo Scientific) into the batch reactor. The reaction mixture represents a trimethylbenzene (TMB): DBE molar ratio of approximately 37:1. Aliquots of the reaction mixture were collected using a 6" needle at 2, 5, 10, 20, and 30 minutes, and then, filtered with 0.2 μm PTFE filters (VWR) to capture solid catalyst before being refrigerated to further quench the reaction and store the mixture for subsequent analysis. Reaction times were chosen to maintain differential conversions (TMB conversion <0.1%) and minimize effects of deactivation to facilitate kinetic analysis. Reaction aliquots were analyzed using gas chromatography (GC, Agilent 7890B) equipped with an Agilent DB-WAX polar column (30 m × 320 μm × 0.5 μm) for component (TMB, DBE, BA, TMB2B) separation before peak area quantification using a flame ionization detector (FID) to determine the concentration of each reagent relative to TMB since it makes up the majority (> 98%) of the liquid mixture throughout the course of the reaction where its conversions are also kept very low (< 0.02%). A small amount (～0.0002 cm^3) of each reaction aliquot was manually injected into the GC using a glass syringe (0.001 cm^3, Agilent) with ～30 rinses in a methanol/acetone solvent mixture (50/50 vol/vol) between injections.

1.4. Propene oligomerization kinetic studies

Propene reactions were performed in a stainless-steel reactor (9.5 mm I.D.) equipped with a concentric thermowell (K-type thermocouple) extending through the axial center of the reactor with the tip in the center of the catalyst bed to monitor temperature. This reactor was supported within a furnace to control the temperature. A physical mixture of these particles and SiO_2 (180–250 μm, Sigma Aldrich, high purity grade) in zeolite/SiO_2 weight-ratios of 0.08–0.20 was prepared

and loaded into the stainless-steel reactor, supported between quartz wool plugs and stainless-steel rods on both sides. Pressure upstream of the catalyst bed was controlled with a back-pressure regulator located downstream. Reactant flows were composed of 75% propylene (99.9%, Matheson), 20% argon (99.999%, Indiana Oxygen), and 5% methane (99.97%, Matheson) used as an internal standard. Reactor effluent flowed through lines heated to 390 K using resistive heating tape (Omegalux) and insulating wrap to a gas chromatograph (Agilent 7890A) equipped with a flame ionization detector (GS GasPro column, 0.320 mm i.d. × 60 m × 0 μm, Agilent) for reactant and product quantification. Reactant space velocity was varied from 6 to 18 mol C_3 $(H^+ s)^{-1}$ by changing both propylene flow rate (4.8×10^{-5})–$(1.1 \times 10^{-4}$ mol/s) and catalyst mass (0.010–0.100 g) at a fixed propylene partial pressure.

Prior to oligomerization, the sample was converted to its H-form using an oxidative pretreatment (1.7×10^{-5} mol s−1 flowing air (air zero, THC <1 ppm) and flowing 5.1×10^{-5} mol s^{-1} Ar (99.999%, Indiana Oxygen)). During the pretreatment, the temperature was ramped to 823 K (0.025 K s^{-1}) and subsequently decreased to reaction temperature (483–523 K). A fresh catalyst was loaded for each experiment unless otherwise noticed. All reported results reflect pseudo-steady-state product formation rates on catalysts, enabling normalization by ex-situ H^+ site counts. Products were quantified with methane as an internal standard with injections beginning after 8–14 minutes time-on-stream. Dimerization rates were estimated from rates of product formation accounting for the formation of products other than dimers as shown in Eq. 4 (main text). A detailed discussion of Eq. 4 is available elsewhere.[8] Absolute uncertainties in rate measurements were estimated by propagating the uncertainties associated with catalyst loading, the initial number of H^+ sites (H^+_0) quantified with NH_3 TPD, and the uncertainty in relative GC peak areas estimated from the fluctuation of the reactant peak area relative to the internal standard peak area in GC

analysis of the reactant stream while bypassing the reactor. Rates are reported at their steady-state values unless otherwise noted. The steady-state rate was taken to be the rate value after dimerization rates changed <4% over 8 ks.

Section S2. X-ray diffraction patterns of MFI samples

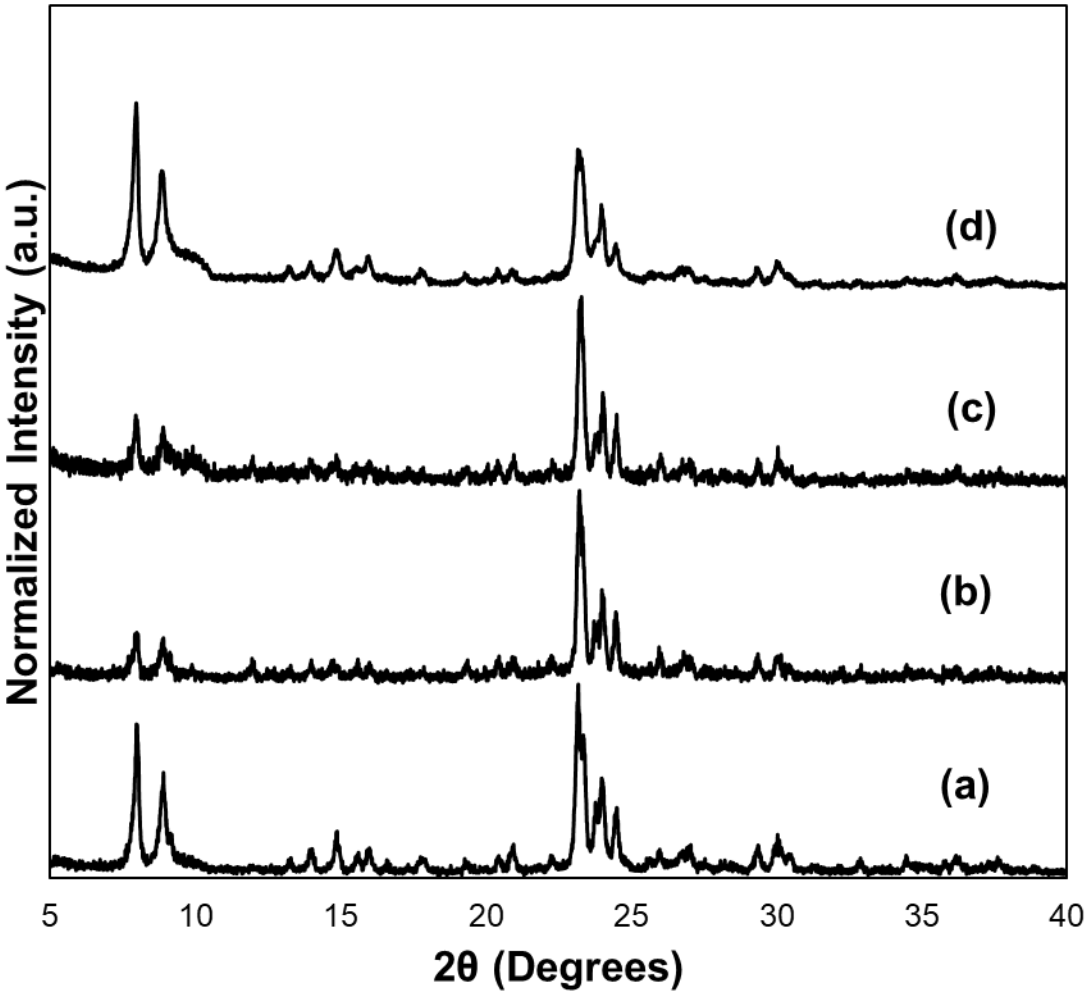

Figure S1. Normalized intensity as a function of 2θ for (a) MFI-208, (b) MFI-183-Z, (c) MFI-158-H and (d) MFI-22-H.

Section S3. N_2 adsorption isotherms for MFI samples

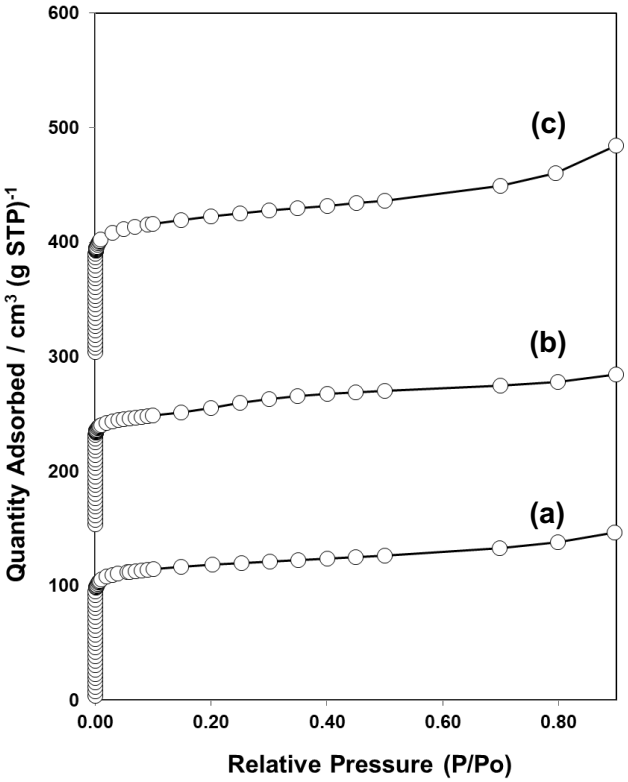

Figure S2. From bottom to top: (a) MFI-158-H, (b) MFI-183-Z and (c) MFI-22-H N_2 adsorption isotherms. The isotherms were vertically offset by 150 cm^3 g^{-1} for clarity.

Section S4. Scanning Electron Microscope and Particle Size Distribution for MFI samples

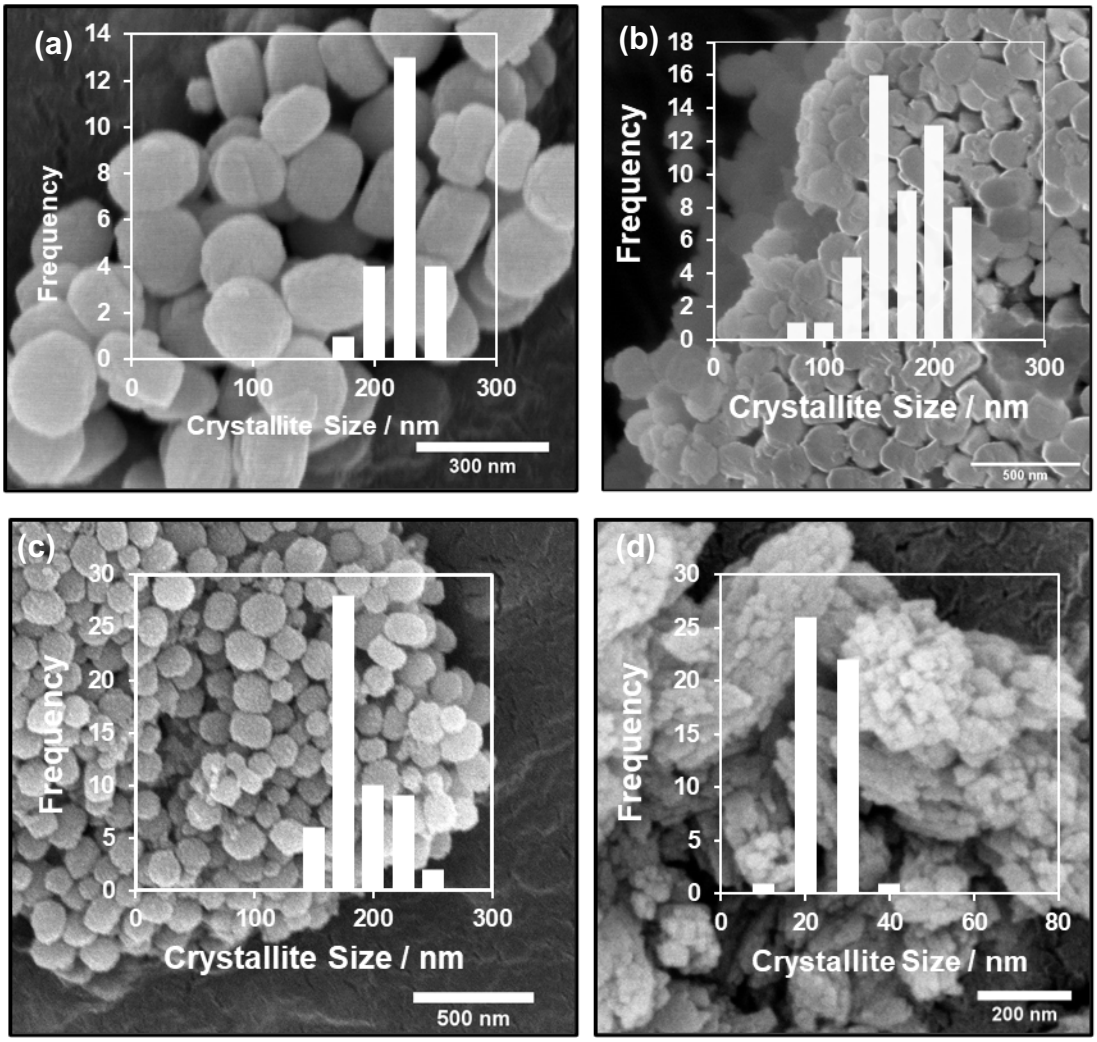

Figure S3. SEM and particle size distribution of (a) MFI-208, (b) MFI-183-Z, (c) MFI-158-H and (d) MFI-22-H.

Section S5. Temperature program desorption profiles for NH_4-form zeolite samples

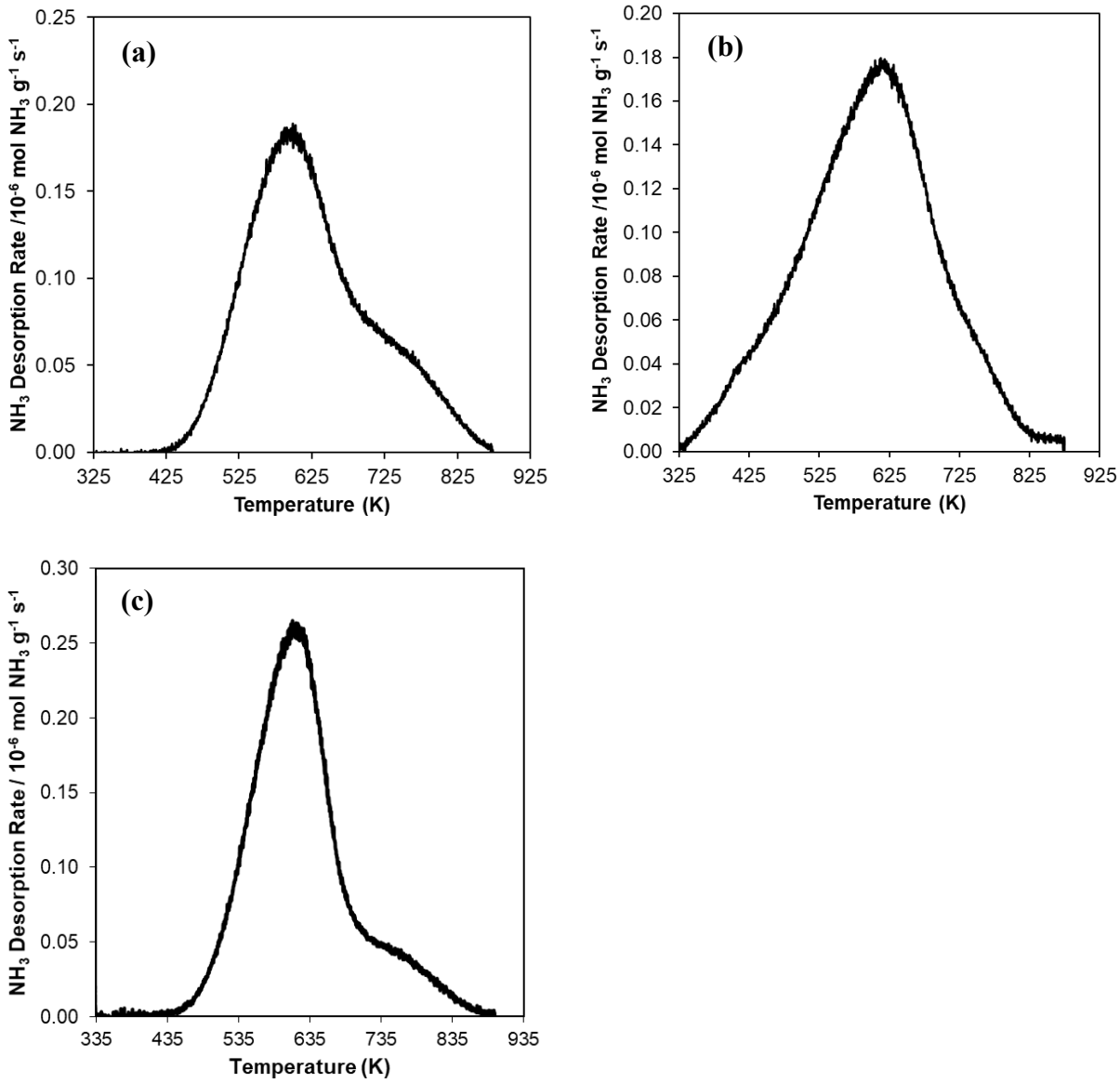

Figure S4. NH_3 TPD profiles for NH_4-form MFI samples (a) MFI-183-Z, (b) MFI-158-H and (c) MFI-22-H.

Section S6. External acid site quantification on MFI by 1,3,5-trimethylbenzene benzylation

On MFI zeolites, mesitylene benzylation occurs only at external H^+ sites and thus was used as a probe reaction to quantify external H^+ sites. The formation rate (per g) of the benzylated product (1,3,5-trimethyl-2-benzylbeznene, TMB2B) is first obtained from the slope of the TMB2B concentration as a function of reaction time (Figure S5). This rate reflects the zero-order rate constant (per g) in the zero order regime. This rate constant (per g) is used alongside the intrinsic zero order rate constant (per H_{ext}^+) to estimate the fraction of external sites. The fraction of external acid sites (H^+_{ext}/Al) was extrapolated from the linear regression calibrated by DTBP titration and desorption method[9] shown in Figure S8.

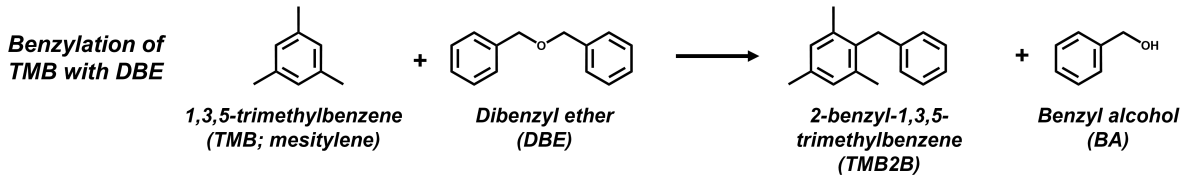

Figure S5. Reaction scheme for benzylation of mesitylene with dibenzyl ether to form 1,3,5 trimethyl-2-benzylbenzene.[9]

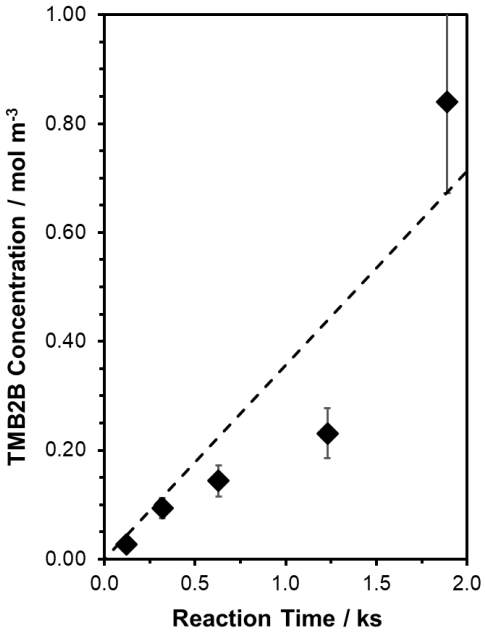

Figure S6. Liquid phase concentration of TM2B as a function of batch reaction time during mesitylene benzylation (363 K) with DBE (TMB : DBE molar ratio = 75:1) on MFI-158-H. Uncertainties in measured concentrations are ±10%.

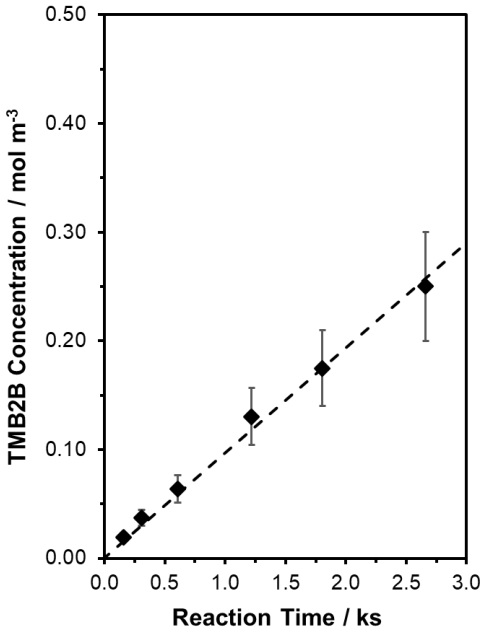

Figure S7. Liquid phase concentration of TM2B as a function of batch reaction time during mesitylene benzylation (363 K) with DBE (TMB : DBE molar ratio = 75:1) on MFI-183-Z. Uncertainties in measured concentrations are ±10%.

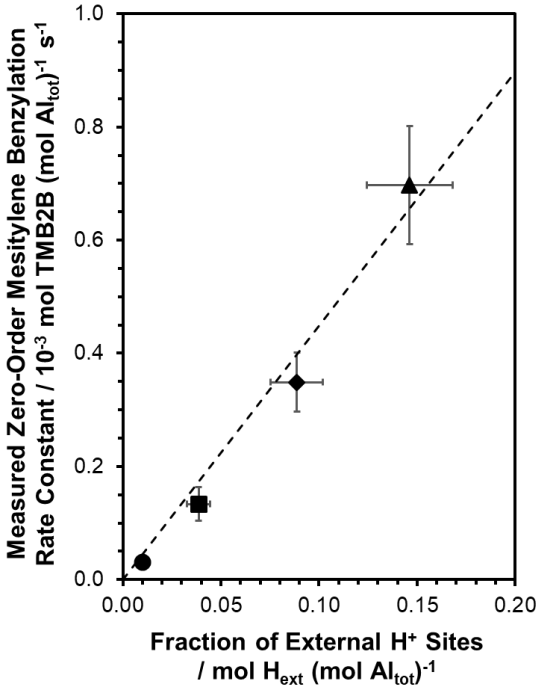

Figure S8. Measured zero-order rate constants (per total Al) for mesitylene benzylation with DBE (363K) as a function of external H^+ sites (per total Al) on MFI-13-P (●), MFI-40-P (■), MFI-C666 (◆) and MFI-C868 (▲) reproduced from Ezenwa, S. et al.[9]. Dashed lines represent the regressed best fits of the data to a linear regression model with zero-intercept.

Table S1. Site characterization of MFI samples (normalized by sample mass)

Sample	k_{TMB2B}[a] / 10^{-3} mol TMB2B (mol Al)$^{-1}$ s^{-1}	H^+_{ext}[b] / 10^{-3} mol H^+_{ext} g^{-1}	H^+_{ext}/Al_{total}
MFI-158-H	0.1596	0.0227	0.042
MFI-183-Z	0.0464	0.0023	0.010
MFI-22-H	0.3489	0.0270	0.078

[a]Rate constants reflect an average or single rate measurement during mesitylene benzylation with DBE (363 K) in the zero-order kinetic regime. Uncertainties range from ±15% to ±30%.
[b]Estimated using the predicted H^+_{ext} content from measured mesitylene benzylation rate constants (per total Al; Figure S8) and the total Al content (per g zeolite). Uncertainties range from ±25% to ±40%.

Section S7. Evaluation of Concentration and Temperature Gradients

Dimerization rates were measured at varied physical dilutions with SiO_2 at fixed reaction conditions on an MFI sample (MFI-158-H) to ensure the absence of bed-scale propene concentration and temperature gradients. Dimerization rates were independent of dilution ratio and space velocity on MFI-158-H at propene pressure (315 kPa C_3H_6, Figure S9), indicating the absence of bed-scale propene concentration and temperature gradients.

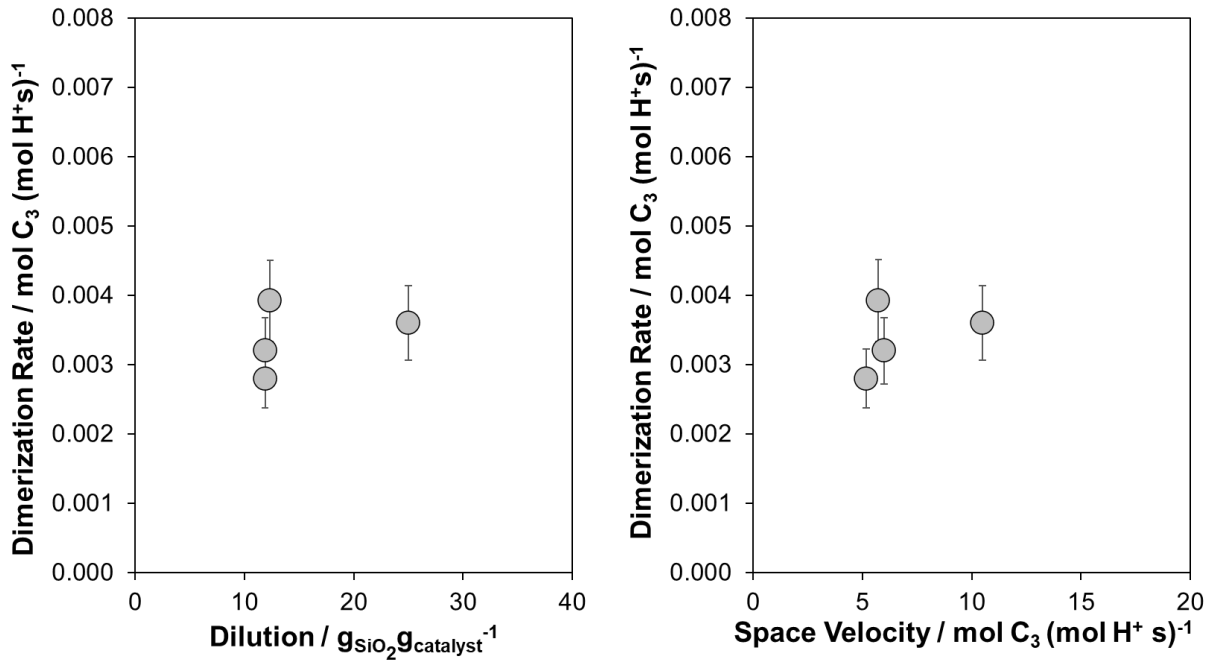

Figure S9. Steady-state propene dimerization rates measured on MFI-158-H at 503 K with varied dilution ratios (left) and varied space velocities (right). Dilution ratios were varied by adjusting SiO_2 or catalyst mass while maintaining fixed space velocity. Space velocities were varied by adjusting catalyst mass or reactant flowrate.

Section S8. X-ray Photoelectron Spectroscopy

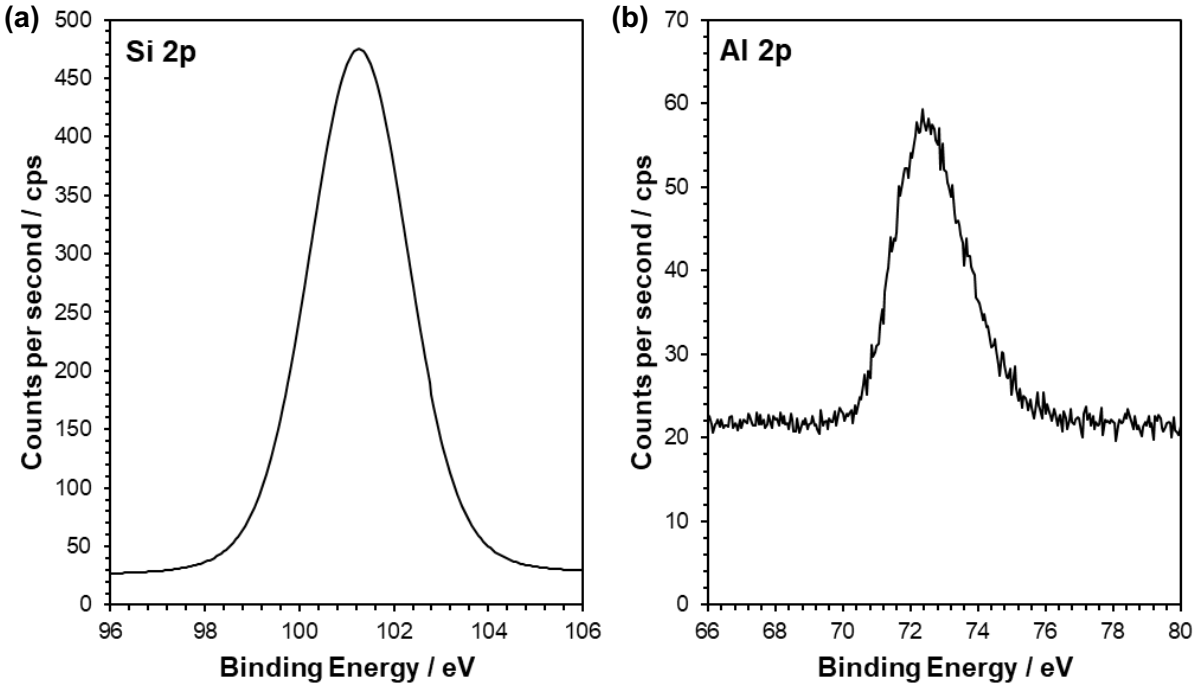

Figure S10. Counts per second of the (a) Si 2p and (b) Al 2p binding energy regions in XPS spectra of MFI-183-Z.

Table S2. Elemental composition of bulk and surface of MFI (up to 10 nm depth)

Sample	Bulk Si/Al_{tot}[a] (ICP)	Surface Si/Al[b] (XPS)
MFI-183-Z	56	8

[a]Uncertainties in ICP quantification are ±10% (unless otherwise noted)
[b]Uncertainties in XPS quantification are ±20%.

Section S9. References

(1) Sun, Y.; Ma, T.; Zhang, L.; Song, Y.; Shang, Y.; Zhai, Y.; Gong, Y.; Duan, A. The Influence of Zoned Al Distribution of ZSM-5 Zeolite on the Reactivity of Hexane Cracking. *Molecular Catalysis* **2020**, *484*, 110770. https://doi.org/10.1016/j.mcat.2020.110770.

(2) Le, T. T.; Shilpa, K.; Lee, C.; Han, S.; Weiland, C.; Bare, S. R.; Dauenhauer, P. J.; Rimer, J. D. Core-Shell and Egg-Shell Zeolite Catalysts for Enhanced Hydrocarbon Processing. *J Catal* **2022**, *405*, 664–675. https://doi.org/10.1016/j.jcat.2021.11.004.

(3) Ghorbanpour, A.; Gumidyala, A.; Grabow, L. C.; Crossley, S. P.; Rimer, J. D. Epitaxial Growth of ZSM-5@Silicalite-1: A Core-Shell Zeolite Designed with Passivated Surface Acidity. *ACS Nano* **2015**, *9* (4), 4006–4016. https://doi.org/10.1021/acsnano.5b01308.

(4) Kim, K.; Ryoo, R.; Jang, H. D.; Choi, M. Spatial Distribution, Strength, and Dealumination Behavior of Acid Sites in Nanocrystalline MFI Zeolites and Their Catalytic Consequences. *J Catal* **2012**, *288*, 115–123. https://doi.org/10.1016/j.jcat.2012.01.009.

(5) Adawi, H. I.; Odigie, F. O.; Sarazen, M. L. Alkylation of Poly-Substituted Aromatics to Probe Effects of Mesopores in Hierarchical Zeolites with Differing Frameworks and Crystal Sizes †. *Cite this: Mol. Syst. Des. Eng* **2021**, *6*, 903. https://doi.org/10.1039/d1me00062d.

(6) Zhang, X.; Liu, D.; Xu, D.; Asahina, S.; Cychosz, K. A.; Agrawal, K. V.; Al Wahedi, Y.; Bhan, A.; Al Hashimi, S.; Terasaki, O.; Thommes, M.; Tsapatsis, M. Synthesis of Self-Pillared Zeolite Nanosheets by Repetitive Branching. *Science (1979)* **2012**, *336* (6089), 1684–1687. https://doi.org/10.1126/science.1221111.

(7) Emdadi, L.; Oh, S. C.; Wu, Y.; Oliaee, S. N.; Diao, Y.; Zhu, G.; Liu, D. The Role of External Acidity of Meso-/Microporous Zeolites in Determining Selectivity for Acid-Catalyzed Reactions of Benzyl Alcohol. *J Catal* **2016**, *335*, 165–174. https://doi.org/10.1016/j.jcat.2015.12.021.

(8) Bickel, E. E.; Gounder, R. Hydrocarbon Products Occluded within Zeolite Micropores Impose Transport Barriers That Regulate Brønsted Acid-Catalyzed Propene Oligomerization. *JACS Au* **2022**. https://doi.org/10.1021/jacsau.2c00462.

(9) Ezenwa, S.; Hopping, G. M.; Sauer, E. D.; Scott, T.; Mack, S.; Gounder, R. Quantification of Extracrystalline Acid Sites in MFI Zeolites after Post-Synthetic Treatments Using Mesitylene Benzylation Kinetics. *React Chem Eng* **2024**. https://doi.org/10.1039/D3RE00589E.